Force ripple reduction methods for tubular permanent magnet linear machines

Alireza Ashouri-Zadeh [a], **Zahra Nasiri-Gheidari** [b,*]

a. *School of Electrical and Computer Engineering, University of Hormozgan, Bandar-Abbas, Iran.*
b. *School of Electrical Engineering, Sharif University of Technology, Tehran, Iran.*

Abstract. This paper presents some novel force ripple reducing techniques for Tubular Permanent-Magnet Linear Machines (TPMLMs) with the square-shaped cross section. These methods are very straightforward, so their implementation in TPMLMs with the square cross section is easy. An analytical form of machine parameters such as the thrust force is obtained by solving the analytical field. A modular configuration for Permanent-Magnet (PM) pole is used to reduce teeth cogging force. Furthermore, the manufacturing cost of TPMLMs can be reduced by using modular pole PM. In this method, the width of PMs is calculated by using Fourier analysis and a sensitivity analysis has been conducted to identify the robustness of this technique. Additional stator side methods are used to decrease the end face cogging force. Moreover, the stator teeth shifting method is proposed to reduce the electromagnetic force ripples. Also, the produced electromagnetic force of the machine is increased by using a delay in the power supply. 3D non-linear finite-element analyses and experimental tests are performed to investigate the effectiveness and performance of proposed techniques.

1. Introduction

Nowadays, interests in Linear Permanent Magnet (LPM) machines and their applications have been increased. The LPM machines are being used in many applications such as vehicle suspension systems, wave energy conversion, active industrial pumps, and robots. The LPM machines thrust force is applied directly to the load without the need to use mechanical gears and transmission system to transform rotary motion into linear motion, which results in a higher dynamic performance, improved reliability, and higher efficiency [1,2]. Among different LPM types, Tubular Permanent-Magnet Linear Machines (TPMLMs) have interesting characteristics. TPMLMs with the simple structure and convenient control, has been paid extensive attention in the field of compressors and industry applications. The thrust force density and efficiency of these machines make them an attractive candidate for applications in which dynamic performance and reliability are important. These machines are more favorable than many conventional LPM machines [3,4]. Also, they have no end windings in the stator and

---

*. *Corresponding author*
E-mail address: znasiri@sharif.edu (Z. Nasiri-Gheidari)

they have no attraction force between their stators and moving parts that means there is zero radial force on the mover. Therefore, the TPMLMs are proper choices for direct-drive applications. Due to high trust density and excellent servo characteristics, TPLMLs are better choices than conventional linear machines for many applications such as vehicle suspension systems, refrigerator compressors, and the elevator door. Besides, TPMLMs are widely used for generators installed inside buoys for wave energy conversion and generators in renewable marine application [5–7].

The TPMLMs depending on the stator structure can be classified into slot-less and slotted machines. The best advantage of the slotted TPMLMs is their higher force density with respect to the slotless ones, but due to the interaction between the Permanent Magnets (PMs) and the stator teeth of slotted TPMLMs, they have a cogging force component. Moreover, in the TPMLMs which stator is shorter than their rotor, due to the interaction between the PMs and the stator end faces, there will be another cogging force component which known as the end faces cogging force. These undesirable forces cause vibration, noise, and higher force ripple, as well as the deterioration of speed and position controls characteristics [8]. Therefore, the force ripple increases as well as force density improves. To overcome these difficulties, various methods are proposed to increase the force density and decrease the produced electromagnetic force ripples [9-29].

A high force density tubular LPM motor is designed and constructed in [9,10]. In [11] a magnetic gear is integrated with a tubular linear machine to improve the thrust force density and enhance the machine efficiency. Various techniques are proposed to reduce teeth cogging force in PM motors. calculation of the optimum PM width is proposed in [12,13]. Also, PM dividing and PM skewing are presented in [14,15]. Moreover, slots shaping and skewing [16,17], PM segmentation [30], selecting the optimum machine parameters [18–21], auxiliary poles utilizing [22], and pole shifting [23] are proposed to decrease the teeth cogging force. For the sake of minimizing the end faces cogging force in the LPM machines, various methods are proposed, such as selecting optimum length for the stator [24,25], end face skewing or stepping [26,27], and end face shifting [29]. Besides, in [29], the slot cogging force is eliminated by the displacement between the upper and left side PM arrays which result in produced electromagnetic force reduction. Some of these methods will result in a reduction of the average force and some other may increase the manufacturing cost and are difficult to perform.

In this paper, TPMLMs with square-shaped cross section are studied and various methods are presented to reduce cogging forces and produced force ripples and improve the produced electromagnetic force. In this paper, the modular pole technique and stator teeth shifting method are used to decrease the undesirable slot cogging force. These methods not only reduce the undesirable force also reduce the manufacturing cost due to reducing the usage of high-quality PMs. Besides, in this paper, the supply phase shifting technique is utilized to improve the produced electromagnetic force. The main contributions of this paper are as follows:

- *The modular pole technique:* To reduce the force ripples and decrease the harmonic content of PMs magnetic fields, modular pole technique is utilized. Comparing this method with other methods like PM skewing [15] illustrates that this method reduces not only undesirable force, but also the manufacturing cost due to reducing the usage of high quality PMs. In this technique, the 2nd, 3rd and 6th harmonic components are reduced significantly;

- *The stator teeth shifting method:* This method is utilized to reduce the high frequency force ripples which are created by stator teeth attraction forces. In this technique, the 3rd harmonic components is reduced. The implementation of this method unlike other similar methods such as teeth skewing and PM shifting [29,31] is straightforward and inexpensive;

- *The supply phase shifting technique:* Although using the previously mentioned proposed techniques reduces force ripples, it leads to decrease the magnitude of produced electromagnetic force. So, the supply phase shifting technique is utilized to improve the produced electromagnetic force;

- *3D finite element analysis:* In order to investigate the effect of proposed methods, 3D finite element analyses of the proposed methods are performed and results are compared with conventional techniques.

Moreover, this paper utilized additional stator side method to reduce the undesirable end faces force. This method is also proposed in [29]. These techniques are straightforward and inexpensive, so they can be implemented in the TPMLMs easily.

With the advancement in computer systems, the Finite Element Method (FEM) could be utilized for modeling of electromagnetic devices [32,33]. The effectiveness of these methods and their performance in the reduction of produced force ripples are evaluated by 3D non-linear finite element analysis and experimental tests. It should be noted that these methods are implemented on the structure of TPMLMs and they dont need to any hardware measurement.

The proceeding sections of this paper are organized as follows: in Section 2, TPMLMs with square-shaped cross section are introduced and their analytical models are presented. The modular pole technique for teeth cogging force reduction is explained in Section 3. The additional stator side method is described

in Section 4. In Section 5, the stator teeth shifting method is explained. Section 6 provides the supply phase shifting technique which is used to increase the produced electromagnetic force. Eventually, the paper is concluded in Section 7.

2. Tubular Permanent Magnet Linear Machine (TPMLM)

Due to high force density and low manufacturing cost, TPMLMs are more popular and they are proposed to be used in many applications such as compressing and suspension. Figure 1(a) shows a typical TPMLM which is studied in this paper. The stator of the TPMLM is multi-sectional and constructed with solid iron slices. As shown, each TPMLM consists of four sections which their construction is simple. After construction, four sections stick together and create the square-shaped stator. The TPMLM mover includes solid iron and PM arrays. Figure 1(b) shows the upper side view of the TPMLM where h, g_e, τ_p, and τ_s are PM thickness, modified air gap length, pole pitch, and slot pitch respectively. As shown in Figure 1(a) and (b), the interaction between magnetic field of mover permanent magnet arrays and stator coils generate the electromagnetic force. The produced electromagnetic force depends on the amplitude of the stator coil current. Due to their square shaped, the analytical analysis of these machines is straightforward. In this structure, PM arrays create similar magnetic field distribution in all air gaps. Therefore, by calculating flux density in one air gap of TPMLM, the other air gap flux density can be obtained easily. The magnetization

function of upper side PM arrays is shown in Figure 1(c) in which, τ_p and $\alpha\,\tau_p$ are pole pitch and PM width respectively. In this figure, the magnetic field sign shows the direction of PMs magnetic field. In this machine, each magnetic field affects only its corresponding air gap, since the produced magnetic potential (A) and magnetic field (B) in other air gaps are negligible. Therefore, calculation of A and B in one side of TPMLMs is similar to their calculation in conventional LPMs. The magnetic flux density of one TPMLM side is obtained as [34]:

$$B_y = - \sum_{n=1,3,\dots}^{\inf} \frac{n\pi}{\tau_p}\, K_B\, e^{\frac{-n\pi g_e}{\tau_p}}\, \cos\left(\frac{n\pi z}{\tau_p}\right), \qquad (1)$$

where

$$K_B = 2\frac{\frac{4\tau_p B_r}{n^2 \pi^2}\, \sin\left(\frac{n\pi\alpha}{2}\right)}{1 + e^{\frac{-n\pi g_e}{\tau_p}} + \frac{\mu_M\left(1 + e^{\frac{-n\pi g_e}{\tau_p}}\right)\left(1 + e^{\frac{2n\pi h}{\tau_p}}\right)}{\mu_0\left(e^{\frac{2n\pi h}{\tau_p}} - 1\right)}}. \qquad (2)$$

The electromagnetic force density of this machine can be calculated as [34]:

$$F = W N_c \int_{-\tau_c/2 - b_0/2}^{\tau_c/2 + b_0/2} J \times B\, dz$$

$$= \sum_{n=1,3,\dots} \frac{4W N_c i K_B n\pi}{\tau_p} e^{\frac{n g_e \pi}{\tau_p}} \sin\left(\frac{n\pi}{\tau_p} z_1\right) \sin\left(\frac{n\pi\tau_c}{2\tau_p}\right), (3)$$

where g_e and J are the modified air gap length and current density vector, μ_0 and μ_M are the magnetic
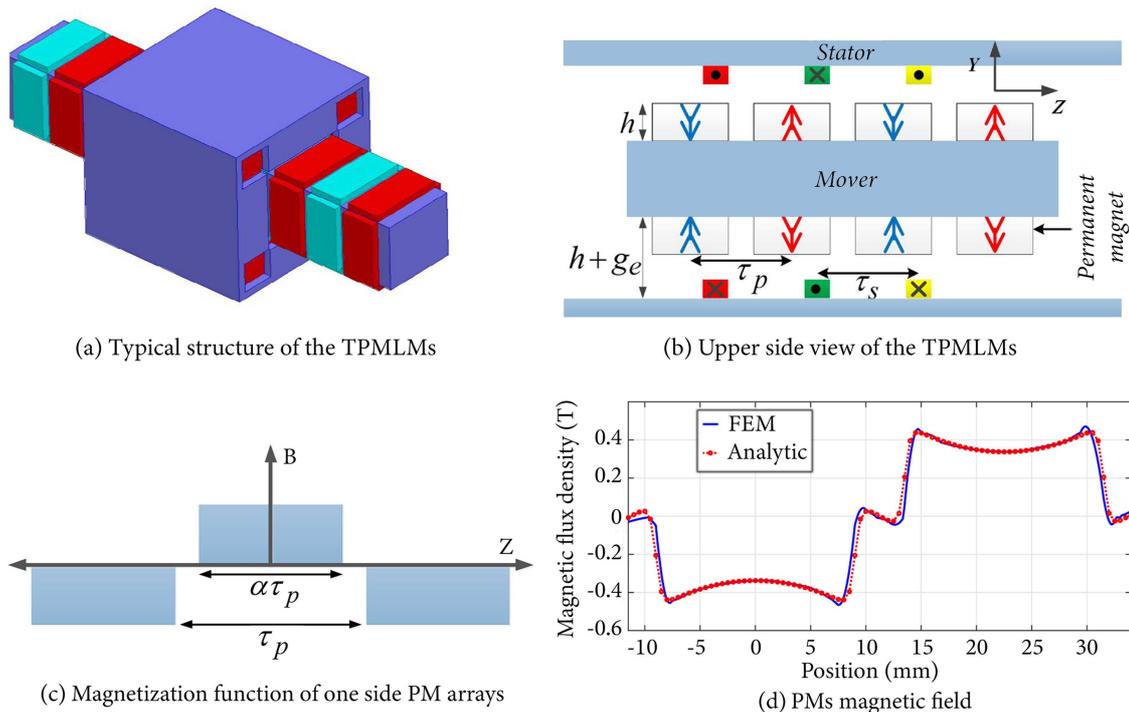

(a) Typical structure of the TPMLMs

(b) Upper side view of the TPMLMs

(c) Magnetization function of one side PM arrays

(d) PMs magnetic field

Figure 1. Fisrt TPMLMs structure.

(a) One stator side of the TPMLM

(b) Rotor and stator of the TPMLM and additional stator side method
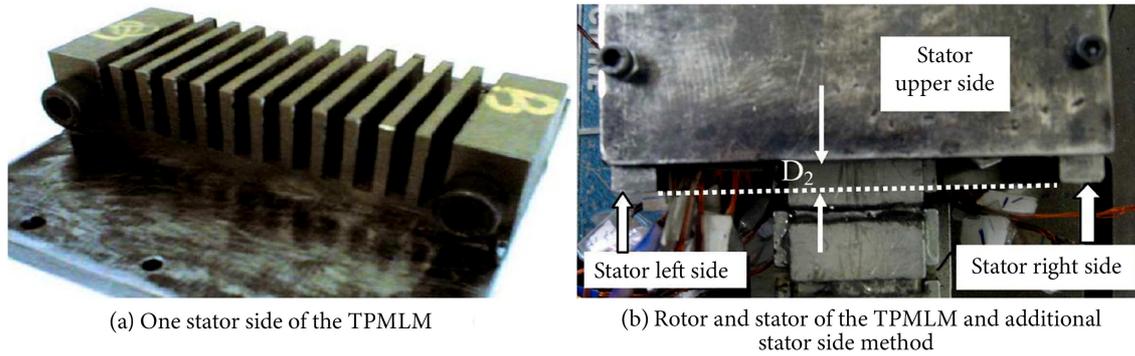
Figure 2. Experimental prototype of the TPMLM [29].

Table 1. TPMLM parameters [29]

Symbol	Dimension	Description
P	4	Pole pairs
g	1 (mm)	Physical air gap length
h	4 (mm)	PM thickness
h_t	17 (mm)	Slot depth
h_g	4 (mm)	Back iron thickness
i	12 (A)	Current amplitude
v	1 (m/sec)	Mover mechanical speed
B_r	1.1 (T)	Remnant magnet
PM	NdFeB	Material
b_0	3.75 (mm)	Opening slot
N_c	24	Turn of one coil
α	0.8	PM length to pole pitch ratio
β	0.48	High quality PM length to pole pitch ratio
W	40 (mm)	Rotor or PM width
τ_c	22.5 (mm)	Coil pitch
τ_p	22.5 (mm)	Pole pitch
τ_s	7.5 (mm)	Slot pitch
q	1	Slot/pole/phase
M	3	Number of phases
μ_0	$4\pi 10^{-7}$ (H/m)	Magnetic permeability of free space
μ_M	1.05 μ_0 (H/m)	Permeability of the PM

permeability of free space and permeability of PM respectively. The relation between fictitious g_e and g is remarked with the aid of Carter coefficient $k_c > 1$ [35]. Designed parameters of this machine are the optimum values to achieve maximum magnetic force density. These parameters are presented in [29] and are given in Table 1.

Figure 1(d) shows air gap flux density magnitude due to PMs for this machine. Comparison between FEM result and analytical result demonstrates appropriate agreement between analytical and FEM result.

Figure 2 shows the real implementation of the TPMLM which is presented in [29]. As shown in Figure 2(b), [29] used additional stator side method to reduce the end faces cogging force. D_2 is the displacement between upper and lateral stator sides. As expressed, the TPMLM stator consists of four similar separated slides.

The worst disadvantages of the TPMLMs are high teeth cogging and end faces cogging forces. These undesirable forces cause TPMLMs to create a non-sinusoidal electromagnetic force. As shown in Figure 3(a), due to cogging and ending forces, produced
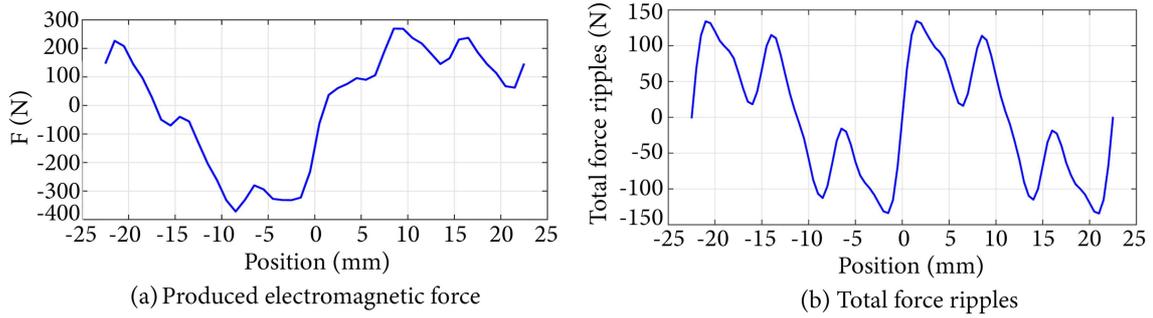
(a) Produced electromagnetic force

(b) Total force ripples

Figure 3. Forces diagram.

electromagnetic force is non-harmonic. Figure 3(b) illustrates the undesirable forces. As shown, the undesirable forces are comparable in magnitude to the produced electromagnetic force. It should be mentioned that the produced electromagnetic force depends on the amplitude of the stator coil currents, amplitude of the flux linkage and the angle between these two vectors (γ). In the normal operation conditions, the amplitude of stator coil current is 12 A (8.5 A rms) and is produced by three phases balanced currents. Hence, the produced electromagnetic force depends only on the angle γ. In all simulation and experimental tests, the current phase and amplitude are fixed on the nominal values and produced force is measured in different mover position (i_a=12 A, i_b=i_c=-6 A dc and to change the γ mover position is displaced). Therefore, the electromagnetic force will have a sinusoidal trend. Moreover, to verify the effectiveness of the proposed force ripple reduction techniques, more finite-element analyses at various load conditions (half and two-thirds load conditions) will be provided. Hence, the stator currents for half and two-thirds load conditions are $i_a = 6$ A, $i_b = i_c = -3$ A and i_a=8 A, i_b=i_c=-4 A respectively.

In this paper, three methods are used to reduce produced force ripples. These methods consider the manufacturing constraint and manufacturing cost.

3. Modular pole technique

The magnetic field distribution of the PM poles has a significant effect on PM machine thrust and its shaping is important in any machine design. Many studies proposed different methods to make a sinusoidal magnetic field distribution. In this method, two types of PMs are used to reduce the produced force ripples of the TPMLMs by reducing the Total Harmonic Distortion (THD). This method reduces not only undesirable force but also the manufacturing cost. As shown in Figure 1(d), there is a flat region at the top of the magnetic field distribution which results in more harmonics in the magnetic field distribution and unwanted performance of the TPMLM. It illustrates that producing a stronger magnetic field in the middle of the pole

by using a stronger or higher quality PM may shape a more sinusoidal magnetic field distribution. Figure 4(a) shows this approach which uses two different PM materials with the same height instead of one. In this figure, $\beta\tau_p$ is the width of higher quality PM and $\frac{(\alpha-\beta)\tau_p}{2}$ is the width of two lower quality PMs. The outside PM modules are made of a lower quality PM material with a weaker magnetization (0.6 tesla), while the middle PM module is made of a higher quality PM material with a stronger magnetization. The magnitude of produced electromagnetic force and THD depend on the width of higher and lower quality PM. Now, the magnetic flux density of one TPMLM side is obtained as [4]:

$$B_y = - \sum_{n=1,3,\ldots}^{\inf} \frac{n\pi}{\tau_p} \left(K_{B1} + K_{B2}\right) e^{\frac{-n\pi g_e}{\tau_p}} \cos\left(\frac{n\pi z}{\tau_p}\right), \quad (4)$$

where

$$K_{B1} = 2 \frac{\frac{4\tau_p B_{r1}}{n^2\pi^2} \sin\left(\frac{n\pi\alpha}{2}\right)}{1 + e^{\frac{-n\pi g_e}{\tau_p}} + \frac{\mu_M(1+e^{\frac{-n\pi g_e}{\tau_p}})(1+e^{\frac{2n\pi h}{\tau_p}})}{\mu_0(e^{\frac{2n\pi h}{\tau_p}}-1)}},$$

$$K_{B2} = 2 \frac{\frac{4\tau_p B_{r2}}{n^2\pi^2} \sin\left(\frac{n\pi\beta}{2}\right)}{1 + e^{\frac{-n\pi g_e}{\tau_p}} + \frac{\mu_M(1+e^{\frac{-n\pi g_e}{\tau_p}})(1+e^{\frac{2n\pi h}{\tau_p}})}{\mu_0(e^{\frac{2n\pi h}{\tau_p}}-1)}}. \quad (5)$$

Parameter β is the width of higher quality PM with stronger magnetization and α is total width of lower and higher quality PMs. For the force ripple reduction, THD of PM magnetic field must be minimized. Therefore, a global search is performed to find optimal values for α and β. The global search algorithm finds optimum design by trying all possible values of α and β. The global search algorithm is particularly robust and rarely gets trapped in local minima. Figure 4(b) shows THD curves of the PMs magnetic field. As shown, region A is the best region for α and β. Center of this region is $\alpha = 0.86$ and $\beta = 0.48$.

In this method, α is more than β. If α and β values are in region B, THD of the PMs magnetic field would be low, but in this region, the first harmonic
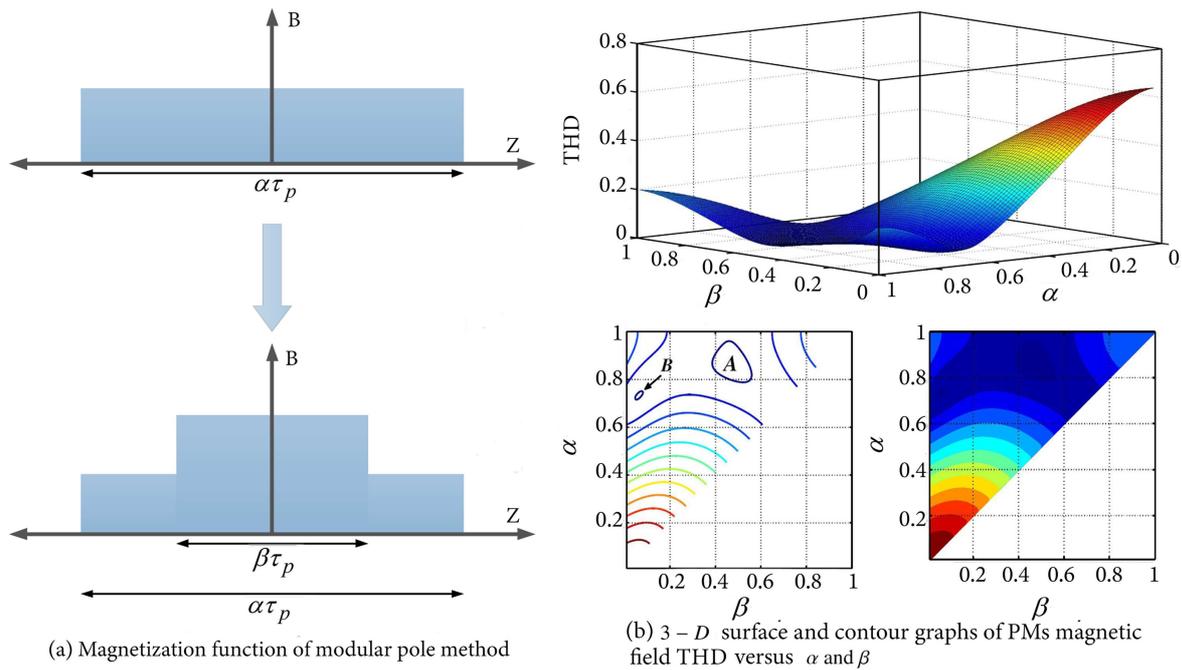
(a) Magnetization function of modular pole method
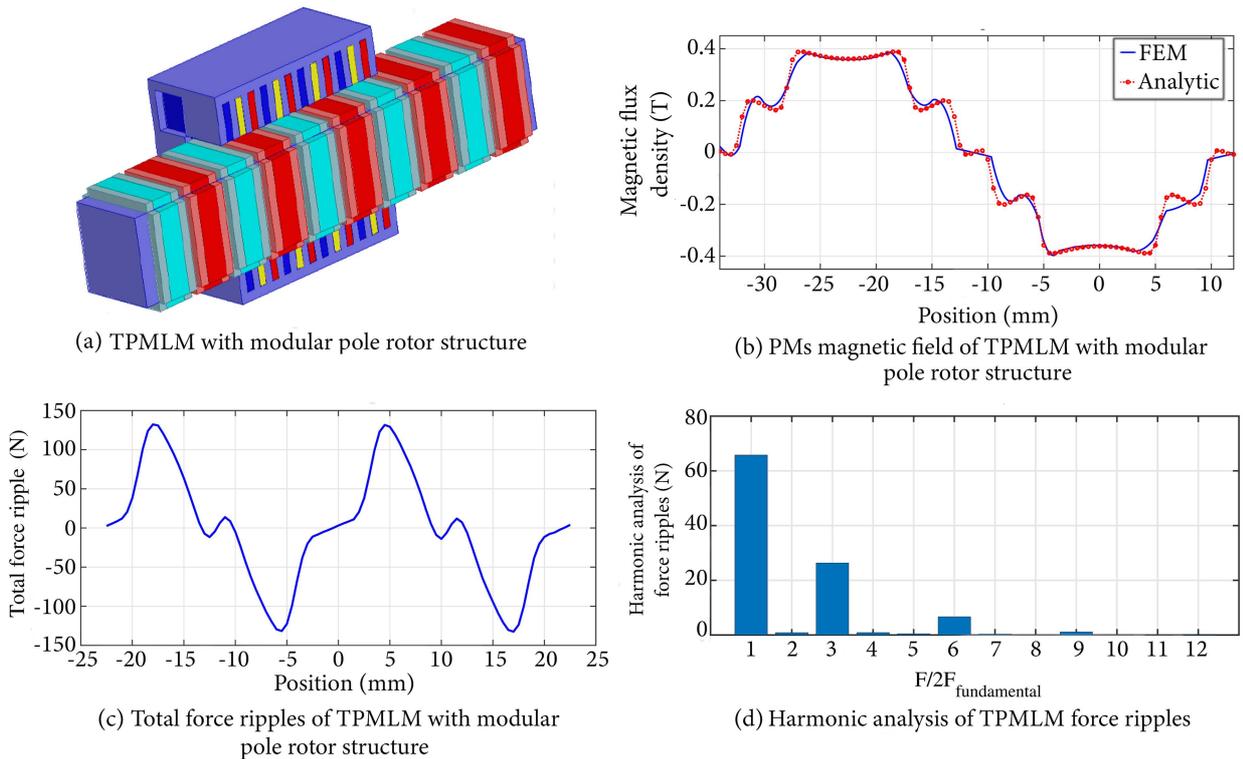
(b) $3 - D$ surface and contour graphs of PMs magnetic field THD versus α and β

Figure 4. Modular pole optimization.

(a) TPMLM with modular pole rotor structure

(b) PMs magnetic field of TPMLM with modular pole rotor structure

(c) Total force ripples of TPMLM with modular pole rotor structure

(d) Harmonic analysis of TPMLM force ripples

Figure 5. Modular pole method.

magnitude of the PMs magnetic field would be low too. Lower first harmonic magnitude causes lower produced electromagnetic force, so the region A presents the best values of α and β. In a region with higher α or β, although produced electromagnetic force increases but THD increases too. In this method, about 40% of high quality PM is slaked and lower quality PM is used instead of high quality one which causes to reduce the manufacturing cost. Besides, Table 2 demonstrates the detailed data about the volume of the utilized PMs. It can be concluded that total PM cost of TPMLM with modular pole is less than original TPMLM.

Figure 5(a) and (b) show the TPMLM with modular pole rotor structure and its PMs magnetic

field respectively. Comparison between FEM result and analytical result demonstrates appropriate agreement between analytical and FEM result. The produced force ripples of TPMLM with modular pole rotor structure is shown in Figure 5(c). The comparison of the produced force ripples (Figure 5(c) and Figure 3(b)) illustrates that although teeth cogging force is reduced properly, end faces cogging force is not declined enough. Figure 5(d) illustrates the harmonic contents of the produced force ripples and it expresses that 1st and 3rd harmonic components (odd harmonics) have the highest amplitude. In this figure, $F_{\text{fundamental}}$ is the power supply frequency. It should be noted that the fundamental frequency of the force ripple harmonics is twice as high as produced electromagnetic force fundamental frequency ($F_{\text{funalmental}_{\text{ripple}}} = 2\,F_{\text{funalmental}_{\text{force}}}$). Therefore, the odd harmonic contents of force ripples are not presented in the harmonic analyses. Since to produce a sinusoidal force, all harmonic components of force ripple should be eliminated.

In this paper, additional stator side method is used to slake the end faces cogging force.

4. Additional stator side method

The end faces cogging force is a dc unidirectional attractive force between stator body and rotor PMs or rotor body and stator PMs. in this definition, left end faces of the stator pull rotor in the right direction and right end faces of the stator pull rotor in the left direction. The dc component of the right stator end faces may eliminate the left ones, because they are equal. Since assuming the cogging force of the two sidelong stator end faces as Eq. (6) and the cogging force of the upper and lower stator end faces as Eq. (7), Eq. (6) gives the total TPMLM end faces cogging force [29].

$$F_1(x) = \sum_{n=1,\ldots} f_{1n} \sin\left(\frac{2n\pi}{\tau_p}x + \theta_0\right), \qquad (6)$$

$$F_2(x) = \sum_{n=1,\ldots} f_{1n} \sin\left(\frac{2n\pi}{\tau_p}(x+d) + \theta_0\right), \qquad (7)$$

$$F_T = F_1 + F_2$$

$$= \sum_{n=1,\ldots} 2f_{1n} \sin\left(\frac{2n\pi}{\tau_p}\left(x+\frac{d}{2}\right)+\theta_0\right)\cdot\cos(\frac{n\pi}{\tau_p}d). \quad (8)$$

As shown in Figure 6(a), d is displacement between the lower and sidelong sides of stator end faces. Based on Eq. (8), if F_1 and F_2 include only odd harmonics and d equal to $\tau_p/2$, F_T can be zero, so the end faces cogging force would be eliminated. Harmonic analysis of the TPMLM produced force ripples shows that the dominant harmonic components of produced force ripples are odd harmonics (1st and 3rd). Thus using $d = \tau_p/2$ causes the elimination of all odd harmonic components of the end faces cogging force. Additional stator side method eliminates only odd harmonic components of the TPMLM produced force ripples which are created by end faces forces. This is one of
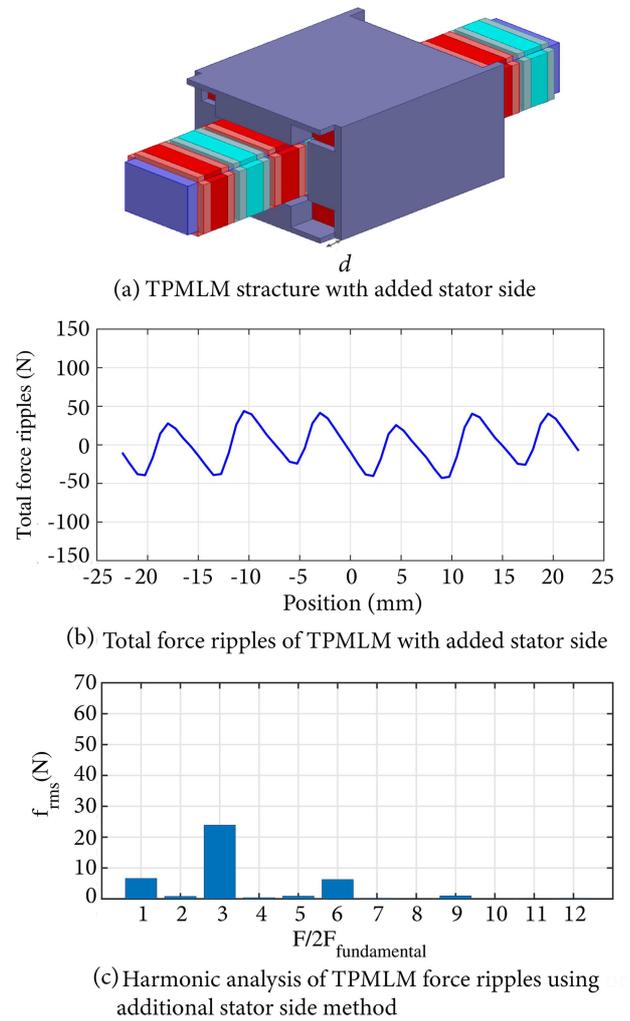

(a) TPMLM stracture with added stator side

(b) Total force ripples of TPMLM with added stator side

(c) Harmonic analysis of TPMLM force ripples using additional stator side method

Figure 6. Additional stator side method.

Table 2. Permanent magnet parameters.

TPMLM type	PM type	B_r (T)	H_c (kA/m)	Length (mm)	volume (mm)^3
Without MP	High quality PM	1.1	1200	720	115200
With MP	High quality PM	1.1	1200	432	69120
	Low quality PM	0.6	700	342	54720

the best methods for decreasing the end face cogging force and was proposed in [29]. Due to its efficiency, the additional stator side method is used to eliminate this component of the total force ripple.

Figure 6(b) illustrates the produced force ripples of TPMLM with this method; The produced force ripples are reduced significantly and end faces cogging force is decreased by around 70%. Figure 6(c) shows the harmonic analysis of the TPMLM produced force ripples and it illustrates that although the first harmonic component is reduced by 90%, the 3rd harmonic component is only decreased by 10%. The harmonic analyses show that only a small amount of 3rd harmonic component of TPMLM produced force ripples belongs to end faces cogging force and most of it is not created by end faces force. The wavelength of the 3rd harmonic of the produced force ripples is equal to τ_s. Hence it can be inferred that this harmonic component depends on stator teeth mostly.

In the next part, stator teeth shifting method is used to decrease the 3rd harmonic component of the produced force ripples.

5. Stator teeth shifting method

Similar to end faces cogging force, teeth cogging force is a dc unidirectional attractive force. The variable reluctance of the path along the TPMLMs air gap creates this undesirable force. In TPMLMs, it is possible to compensate this variable reluctance by displacement of the upper and lower teeth of the stator. As expressed in Section 2, the stator of TPMLMs consists of four separate parts (sides). The stator Teeth shifting method could be implemented by displacement of the upper and lower parts (or two lateral parts). The implementation of the stator teeth shifting method is shown in Figure 7(a). As shown, d_2 is displacement between lower and lateral stator teeth. Assuming the cogging force of two lateral stator teeth as Eq. (9) and the cogging force of the lower and upper stator teeth as Eq. (10), the total teeth cogging force of the TPMLM is calculated by Eq. (11):

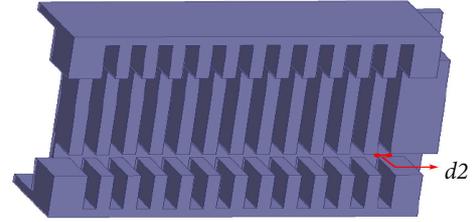$$F_1(x) = \sum_{n=1,\ldots} f_n \sin\left(\frac{2n\pi}{\tau_s}x + \theta_0\right), \qquad (9)$$

where

$$F_2(x) = \sum_{n=1,\ldots} f_n \sin\left(\frac{2n\pi}{\tau_s}(x + d_2) + \theta_0\right), \qquad (10)$$
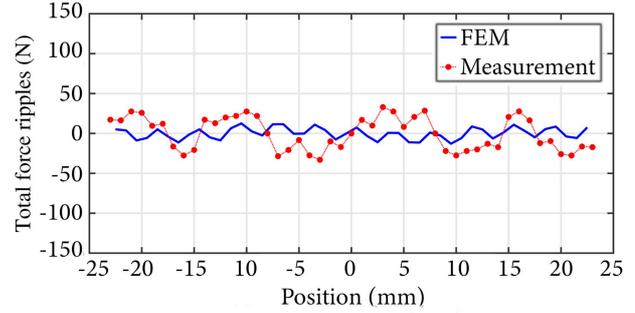
$$F_T = F_1 + F_2$$

$$= \sum_{n=1,\ldots} 2f_n \sin\left(\frac{2n\pi}{\tau_s}(x + \frac{d_2}{2}) + \theta_0\right) \cdot \cos(\frac{n\pi}{\tau_s}d_2). \quad (11)$$
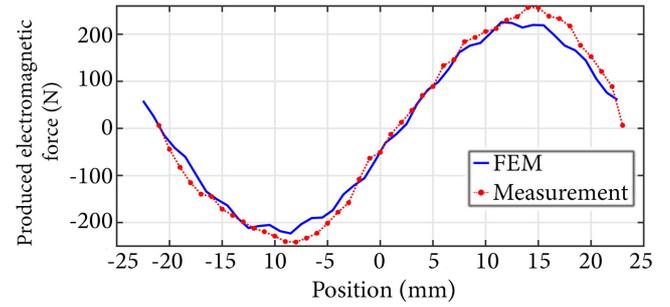
Eq. (11) expresses that if F_1 and F_2 include only odd harmonics and d_2 equal to $\tau_s/2$, F_T can be zero, so

(a) TPMLM stator with shfted teeth

(b) Total force ripples of TPMLM with shifted stator teeth

(c) Produced electromagnetic force of the TPMLM with shifted stator teeth in FEM and measurement produced electromagnetic force

Figure 7. Stator teeth shifting method.

the stator teeth cogging force would be eliminated. Also, harmonic analysis of the TPMLM produced force ripples shows the most harmonic components of the force ripples are odd harmonics (1st and 3rd). Hence using $d_2 = \tau_s/2$ causes the elimination of all odd harmonic components of the produced force ripples which are created by stator teeth cogging force.

Figure 7(b) and (c) illustrate the produced force ripples and produced electromagnetic force of the TPMLM using stator teeth shifting method, respectively. Also, these figures show the results of an experimental test [29]. The experimental test was performed on a TPMLM without considering modular pole technique and the stator teeth shifting method. As shown, the produced force ripples have reduced significantly and the produced electromagnetic force has been more similar to the sinusoidal wave. Moreover, to compare the efficiency of these methods, sensitivity analysis of the produced force ripples are illustrated in Figure 8. As it is shown in this figure, the modular pole technique reduces all harmonic components acceptably except first harmonic. The additional stator technique
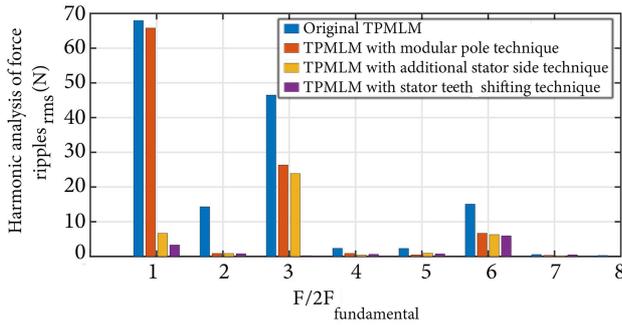
Figure 8. Harmonic analysis of TPMLM force ripples according to different force ripples reduction methods.

Figure 9. Harmonic analysis of produced electromagnetic force with and without power supply shifting.

eliminates only the first harmonic component. The stator teeth shifting technique eliminates 3rd harmonic component completely.

Although teeth shifting method reduces the produced force ripples, it causes reduction of the produced electromagnetic force peak. In this method, the produced electromagnetic forces of the lateral sides have delay compared to the other sides. Therefore, if the produced electromagnetic force of lateral side is considered as Eq. (12), the lower and upper produced electromagnetic force is obtained as Eq. (13). The produced electromagnetic force is the summation of these forces that is defined by Eq. (14):

$$f_{p1}(x) = F_p \sin\left(\frac{\pi}{\tau_p}x\right), \qquad (12)$$

$$f_{p2}(x) = F_p \sin\left(\frac{\pi}{\tau_p}(x + d_2)\right), \qquad (13)$$

$$f_{pT} = f_{p1} + f_{p2} = 2F_p \sin\left(\frac{\pi}{\tau_p}(x + \frac{d_2}{2})\right) . \cos\left(\frac{n\pi}{2\tau_p}d_2\right)$$

$$2\,F_p(\text{new}) \sin\left(\frac{\pi}{\tau_p}(x + \frac{d_2}{2})\right)$$

$$0.96 \times 2F_p \sin\left(\frac{\pi}{\tau_p}(x + \frac{d_2}{2})\right), \qquad (14)$$

where d_2 is the displacement between lower and lateral stator teeth. Eq. (14) expresses that maximum produced electromagnetic force depends on the displacement between lower and lateral stator teeth. In this structure, the maximum produced force is 96% out of original force. Since a new supplying method is proposed to overcome this problem.

6. Supplay phase shifting

Using stator teeth shifting method for the teeth cogging force reduction causes a decrease of the maximum electromagnetic force. To overcome this problem and synchronize the produced electromagnetic force of
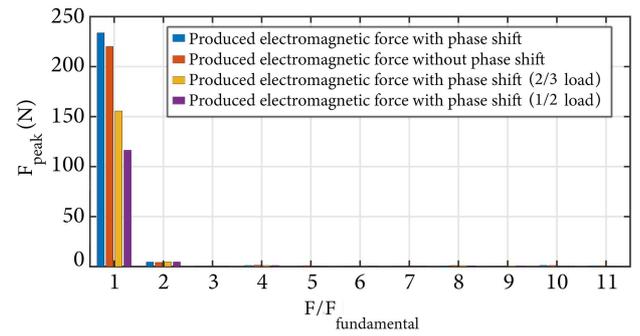
lateral sides with lower and upper sides of the stator, supply phase shifting method is used. In this method, conductors of lateral sides are feed with a delay. To synchronize the forces, the phase difference between two supply currents is:

$$\Delta\phi = \frac{\Delta L}{\tau_s}\pi, \qquad (15)$$

where ΔL is the displacement between lower and lateral stator teeth. In this machine, $\Delta\phi$ is equal to 0.5236 rad. Power supply time delay is obtained by Eq. (16):

$$\text{Power supply time delay} = \frac{\Delta\phi}{2\pi f}. \qquad (16)$$

Figure 9 shows harmonic analysis of the TPMLM produced electromagnetic force with and without this method. As shown, this method increased only the fundamental frequency of the produced electromagnetic force and does not change the other harmonic components. Besides, this figure illustrates the harmonic analysis of the TPMLM produced electromagnetic force with all proposed methods for two another load conditions (half and two thirds load points). As shown, these proposed methods have reduced undesirable forces in these two load points properly. It can be seen that 2nd harmonics are in the same range, therefore, all these proposed methods reduce force ripples independent of load condition.

To investigate the effectiveness of the proposed method in electromagnetic force increase, the produced electromagnetic force obtained analytically is compared with the FEM results and experimental results in Figure 10. Besides, the produced electromagnetic forces for half load level and two-thirds load level are calculated by FEM to verify the performance of force ripple reduction techniques. The modular pole technique and the stator teeth shifting method have not been considered in the experimental test. As shown, the produced electromagnetic force is increased about 5%, and it follows the analytical and measurement values.
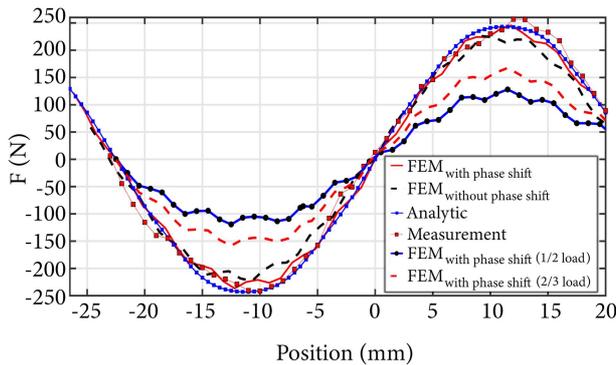
Figure 10. Analytic, FEM, and measurement produced electromagnetic forces.

Proper agreement between the analytical result and the obtained results with FEM simulations verifies the performance of the methods.

7. Conclusion

In this paper, some new methods were presented to reduce the force ripples of the Tubular Permanent-Magnet Linear Machines (TPMLMs). The modular pole method was used to reduce not only the produced force ripples but also manufacturing cost. Global search was used to find optimum Permanent Magnet (PM) widths with minimum Total Harmonic Distortion (THD). This method reduced 2nd, 3rd, 4th, 5th, and 6th harmonic components properly. The additional stator side method was used to reduce the end faces cogging force. this method decreased 1st harmonic component significantly. To decrease the teeth cogging force and the 3rd harmonic component of produced force ripples, the stator teeth shifting method was introduced. All these methods are simple to implement and they don't need additional measurement equipment.

The teeth shifting method reduces the produced electromagnetic force, in order to compensate this reduction, supply phase shifting method was proposed. This method increased the produced electromagnetic force around 5%. The 3D finite-element analysis and as well as experimental measurements have proven the validity of the proposed methods. Some harmonic analyses were performed on these results to illustrate the efficiency of the methods.

Acknowledgment

Funding

Conflicts of interest

The author is an Editorial Board Member/Editor-inChief/Associate Editor/Guest Editor for Scientia Iranica and was not involved in the editorial review or the decision to publish this article.

Authors contribution statement

One of the authors is an Editorial Board Member, of Scientia Iranica and was not involved in the editorial review process or the decision to publish this article.

References

1. Esfahanian, H.R., Hasanzadeh, S., Heydari, M., et al. "Design, optimization, and control of a linear tubular machine integrated with levitation and guidance for maglev applications", *Scientia Iranica*, **30**(4), pp. 1330-1341 (2021).
https://doi.org/10.24200/sci.2021.57416.5231

2. Zare Chavoshi A. and Ganji, B. "Instantaneous thrust control of linear switched reluctance motors with segmental translator", *Scientia Iranica*, **27**(6), pp. 3140–3149 (2020).
https://doi.org/10.24200/sci.2019.51380.2144

3. Kumar, A. and Supare, C. "Design, analysis and realization of tubular linear induction motor for hammering application", *In 2020 IEEE International Conference on Power Electronics, Drives and Energy Systems (PEDES)*, IEEE, pp. 1–7 (2020).
https://doi.org/10.1109/PEDES49360.2020.9379399

4. Zhang, H., Xu, Z., Jin, L., et al. "Electromagnetic calculation of tubular permanent magnet linear oscillation actuator considering corrected air gap permeance", *IEEE Transactions on Magnetics*, **59**(5), 8000305 (2023).
https://doi.org/10.1109/TMAG.2023.3243833

5. Wang, A. "Winding design and optimization of single-phase permanent magnet tubular linear generator for direct-drive wave power generation", *In 2021 13th International Symposium on Linear Drives for Industry Applications (LDIA)*, IEEE, pp. 1–4 (2021).
https://doi.org/10.1109/LDIA49489.2021.9505866

6. Qiu, S., Zhao, W., Zhang, C., et al. "A novel structure of tubular staggered transverse-flux permanent-magnet linear generator for wave energy conversion", *IEEE Trans. Energy Convers.*, **37**(1), pp. 24–35 (2021). https://doi.org/10.1109/TEC.2021.3088722

7. Naghavi, F., Sheshaprasad, S., Gardner, M., et al. "Permanent magnet linear generator design for surface riding wave energy converters",

in *2021 IEEE Energy Conversion Congress and Exposition (ECCE)*, IEEE, pp. 4369–4375 (2021). https://doi.org/10.48550/arXiv.2108.08346

8. Taghipour Boroujeni, S., Emami, S.P., Takorabet, N., et al. "Torque ripple minimization in consequent-pole PM machines using harmonic current injection", *Scientia Iranica*, **32**(5), pp. 1-12 (2025). https://doi.org/10.24200/sci.2022.60312.6725

9. Li, X., Wang, X., and Yu, S. "Design and analysis of a novel transverse-flux tubular linear switched reluctance machine for minimizing force ripple", *IEEE Trans. Transp. Electrif.*, **7**(2), pp. 741–753 (2020). https://doi.org/10.1109/TTE.2020.3033535

10. Mutluer, M. "A new approach to increase the thrust force of tubular linear voice coil motor", *IEEE Can. J. Electr. Comput. Eng.*, **44**(4), pp. 509–515 (2021). https://doi.org/10.1109/ICJECE.2021.3094167

11. Khuong, N.D. and Shimono, T. "Modeling and analysis of a magnetic geared linear motor", *In 2022 International Power Electronics Conference*, IEEE, pp. 260–267 (2022). https://doi.org/10.23919/IPEC-Himeji2022-ECCE53331.2022.9807249

12. Luo, H.-h., Wu, J., and Chang, W.-S. "Minimizing thrust fluctuation in moving-magnet permanent-magnet brushless linear DC motors", *IEEE Trans. Magn.*, **43**(5), pp. 1968–1972 (2007). https://doi.org/10.1109/TMAG.2007.892081

13. Yoshimura, T., Kim, H., Watada, M., et al. "Analysis of the reduction of detent force in a permanent magnet linear synchronous motor", *IEEE Trans. Magn.*, **31**(6), pp. 3728–3730 (1995). https://doi.org/10.1109/20.489752

14. Shabani, M.A., Milimonfared, J., and Taghipour, S. "Cogging force mitigation of tubular per- manent magnet machines with magnet dividing", *In 2007 International Conference on Electrical Machines and Systems*, IEEE, pp. 810–814 (2007). https://doi.org/10.1109/ICEMS12746.2007.4412196

15. Jung, I.-S., Hur, J., and Hyun, D.-S. "Performance analysis of skewed pm linear synchronous motor according to various design parameters", *IEEE Trans. Magn.*, **37**(5), pp. 3653–3657 (2001). https://doi.org/10.1109/20.952683

16. Wang, S., Wang, Y., Liu, C., et al. "Detent force minimization of a tubular flux-switching permanent magnet motor using un-equal width stator slots based on taguchi method", *IEEE Trans. Appl. Supercond.*, **30**(4), 5202505 (2020). https://doi.org/10.1109/TASC.2020.2976068

17. Wang, W., Zhao, J., Song, J., et al. "Thrust performance improvement for PMSLM through double-layer reverse skewed coil and wrf-mkh method", *IEEE/ASME Transactions on Mechatronics*, **25**(6), pp. 2950–2960 (2020). https://doi.org/10.1109/TMECH.2020.3000265

18. Guo, L., Zhou, Q., Galea, M., et al. "Cogging force optimization of double-sided tubular linear machine with tooth-cutting", *IEEE Trans. Ind. Electron.*, **69**(7), pp. 7161–7169 (2021). https://doi.org/10.1109/TIE.2021.3101017

19. Zhao, W., Ma, A., Ji, J., et al. "Multiobjective optimization of a double-side linear vernier pm motor using response surface method and differential evolution", *IEEE Trans. Ind. Electron.*, **67**(1), pp. 80–90 (2019). https://doi.org/10.1109/TIE.2019.2893848

20. Li Z. and Niu, S. "Design of a novel hybrid-excited transverse-flux tubular linear machine with complementary structure", *IEEE Trans. Magn.*, **58**(8), 8105506 (2021). https://doi.org/10.1109/TMAG.2021.3139368

21. Liu, C.-T., Hwang, C.-C., Li, P.-L., et al. "Design optimization of a double-sided hybrid excited linear flux switching pm motor with low force ripple", *IEEE Trans. Magn.*, **50**(11), 8102704 (Nov. 2014). https://doi.org/10.1109/TMAG.2014.2322630

22. Hwang, C.-C., Li, P.-L., and Liu, C.-T. "Design and analysis of a novel hybrid excited linear flux switching permanent magnet motor", *IEEE Trans. Magn.*, **48**(11), pp. 2969–2972 (Nov. 2012). https://doi.org/10.1109/TMAG.2012.2195716

23. Chen, Q., Yan, Y., Xu, G., et al. "Principle of torque ripple reduction in syn- chronous reluctance motors with shifted asymmetrical poles", *IEEE Journal of Emerging and Selected Topics in Power Electronics*, **8**(3), pp. 2611–2622 (2019). https://doi.org/10.1109/JESTPE.2019.2909570

24. Inoue M. and Sato, K. "An approach to a suitable stator length for minimizing the detent force of permanent magnet linear synchronous motors", *IEEE Trans. Magn.*, **36**(4), pp. 1890–1893 (2000). https://doi.org/10.1109/20.877814

25. Deng, C., Ye, C., Yang, J., et al. "A novel permanent magnet linear motor for the application of electromagnetic launch system", *IEEE Transactions on Applied Superconductivity*, **30**(4), 4902005 (2020). https://doi.org/10.1109/TASC.2020.2986732

26. Wang, J., Inoue, M., Amara, Y., et al. "Cogging-force-reduction techniques for linear permanent-magnet machines", *IEE Proceedings-Electric Power Applications*, **152**(3), pp. 731–738 (2005). https://doi.org/10.1049/ip-epa:20045254

27. Li, Z., Niu, S., Zhao, X., et al. "Force ripple reduction of a fractional pole pair complementary modularized variable reluctance linear machine for long stroke application", *IEEE Transactions on Transportation Electrification*, **9**(3), pp. 4613–4625 (2023). https://doi.org/10.1109/TTE.2023.3242077

28. Boff, B.H.B., Eckert, P.R., and Amara, Y. "A comprehensive review on the end effects of linear permanent magnet machines", *IEEE Transactions on Industry Applications*, **59**(2), pp. 1728–1741 (2022). https://doi.org/10.1109/TIA.2022.3230630

29. Boroujeni, S.T., Milimonfared, J., and Ashabani, M. "Design, prototyping, and analysis of a novel tubular permanent-magnet linear machine", *IEEE Trans. Magn.*, **45**(12), pp. 5405–5413 (2009). https://doi.org/10.1109/TMAG.2009.2022837

30. Zamani, V., Taghipour Boroujeni, and Takorabet, N. "Optimum arrangement of pms in surface-mounted pm machines: cogging torque and flux density harmonics", *Electrical Engineering*, **102**(5), pp. 1117–1127 (2020). https://doi.org/10.1007/s00202-020-00925-8

31. Wang, Y., Jin, M., Fei, W., et al. "Cogging torque reduction in permanent magnet flux- switching machines by rotor teeth axial pairing", *IET electric power applications*, **4**(7), pp. 500–506 (2010). https://doi.org/10.1049/iet-epa.2009.0205

32. Saneie, H., Daniar, A., and Nasiri-Gheidari, Z. "Design optimization of a low speed small scale modular axial flux permanent magnet synchronous generator for urban wind turbine application", *Scientia Iranica*, **29**(6), pp. 3326–3337 (2022). https://doi.org/10.24200/sci.2021.56405.4709

33. Bahari, M. and Nasiri-Gheidari, Z. "The comparative analysis of AC-flux and DC-flux resolvers", *Scientia Iranica*, **29**(4), pp. 2007–2013 (2022). https://doi.org/10.24200/sci.2020.55469.4236

34. Gieras, J., Piech, Z., and Tomczuk, B., *Linear Synchronous Motors: Transportation and Au- tomation Systems, Second Edition*, ser. Electric Power Engineering Series. CRC Press, (2011).

35. Gieras, J.F., Wang, R.-J., and Kamper, M. J. *Axial flux permanent magnet brushless machines*, Springer, **1**, (2008).

Biographies

Alireza Ashouri-Zadeh received the BSc degree in Electrical Engineering from Amirkabir University of Technology, Tehran, Iran in 2012, and the MSc and PhD degrees from Sharif University of Technology, in 2014 and 2019, respectively. He is currently an Assistant Professor in the Department of Electrical and Computer Engineering at the University of Hormozgan. His research interests include power system dynamic, power system operation and control, and renewable energy integration.

Zahra Nasiri-Gheidari (Senior member, IEEE) received the BSc degree from the Iran University of Sciences and Technology, Tehran, Iran in 2004 and the MSc and PhD degrees from University of Tehran, Tehran in 2006 and 2012, respectively, all in Electrical Engineering. She is currently an Associate Professor at the Department of Electrical Engineering, Sharif University of Technology. Her research interests include design, optimization, and performance analysis of Electrical Machines and Electromagnetic Sensors.